

## Synthesis and characterization of $\text{CuAl}_2\text{O}_4$ nanoparticles via a reverse microemulsion method

J.Chandradass and Ki Hyeon Kim\*

Department of Physics Yeungnam University Gyeongsan, Gyeongsangbuk-do-712-749 South Korea

Copper aluminate ( $\text{CuAl}_2\text{O}_4$ ) nanoparticles have been synthesized using micro reactors made of Igepal CO520/water/cyclohexane microemulsions. The effect of the water- to- surfactant ratio on the preparation of  $\text{CuAl}_2\text{O}_4$  has been studied. The synthesized and calcined powders were characterized by thermogravimetry-differential thermal analysis (TGA-DTA), X-ray diffraction analysis (XRD) and transmission electron microscopy (TEM). Phase pure  $\text{CuAl}_2\text{O}_4$  was synthesized at 800 °C for 2 h at  $R = 4$ . The average particle size as determined from TEM varies from 10-20 nm. A High resolution TEM (HRTEM) study shows well resolved (220) fringes corresponding to  $\text{CuAl}_2\text{O}_4$ . FTIR analysis was carried out to monitor the elimination of residual oil and surfactant phases from the micro emulsion-derived precursor and calcined powder.

**Key words:** Ceramics, Chemical synthesis, Differential Thermal analysis, Scanning electron microscopy.

### Introduction

Copper (II) aluminate ( $\text{CuAl}_2\text{O}_4$ ) with spinel structure is of interest due to their technological application as ceramic pigments, coatings [1] and catalysts [2-4]. For the synthesis of  $\text{CuAl}_2\text{O}_4$ , methods involving fusion of the two component oxides at high temperatures [5], co-precipitation reactions in solution [4] and a sol-gel technique [6] have been reported in the literature. Among all the chemical processes that were developed for the preparation of fine ceramic powders and for producing a wide array of metals and metal oxide compounds [7-9] microemulsion processing, involving reverse micelles has been demonstrated as a superior method [10] in terms of being able to deliver homogeneous and nanosized grains of a variety of oxides. This aqueous method uses readily available inexpensive, and easily handled precursors of  $\text{Cu}(\text{NO}_3)_2$  and  $\text{Al}(\text{NO}_3)_3$ , and eliminates the extra handling requirements that are usually associated with moisture-sensitive precursors. In recent years, the microemulsion method has been studied and utilized widely and has been a key technique to synthesize oxide nanoparticles which have the characteristics of a well-dispersed, controlled size and narrow size distribution. Recently James *et al.* [11] studied the formation characteristics of both  $\alpha\text{-Al}_2\text{O}_3$  and a  $\text{CuAl}_2\text{O}_4$  spinel from  $\text{Cu}^{2+}$  ion doped boehmite xerogels by systematically varying the doping level and calcinations temperatures. Yanyan *et al.* [12] prepared  $\text{CuAl}_2\text{O}_4$  nanoparticles in the range 10-30 nm by sol-gel autocombustion. Although several methods have been used to synthesize this material, some

improvement or an alternative suitable route is still required to obtain homogenous powders with a smaller particle size at a relatively low temperature for commercial production. However, the synthesis of  $\text{CuAl}_2\text{O}_4$  nanoparticles has not been reported by the microemulsion method. In this study, we present the synthesis of  $\text{CuAl}_2\text{O}_4$  nanoparticles based on an Igepal CO520/water/cyclohexane reverse microemulsion route at 800 °C for 2 h and investigate the effect of the water-to-surfactant ratio. This technique lowered the particle size to the nanometre scale in the range 10-20 nm.

### Experimental Procedure

Typically, microemulsions of a total volume 200 ml were prepared at ambient temperature in a 250 ml vial with rapid stirring; these consisted of 40 ml of nonionic surfactant poly(oxyethylene) nonylphenyl ether (Igepal CO-520, Aldrich Chemical Co., USA), 100 ml of cyclohexane, 6.5-13.2 ml of mixed aqueous solution ( $\text{Cu} : \text{Al} = 1 : 1$ ) and deionized water. The size of the resulting particles was controlled by the ratio  $R = [\text{water}]/[\text{surfactant}]$ . The microemulsion was mixed rapidly, and after 5 minutes of equilibration, 3-6 ml of  $\text{NH}_4\text{OH}$  (28%) (Dae Jung chemicals, Korea) was injected into the micro-emulsion. The microemulsion was then centrifuged to extract the particles, which were subsequently washed with ethanol to remove any residual surfactant. The thermal characteristics of the precursors were determined by thermogravimetry and differential thermal analysis (STA 1500). The phase identification of calcined powders was recorded by an X-ray diffractometer (Philips X'pert MPD 3040). Transmission electron microscopy (JEM 2100F) was performed at an accelerating voltage of 200 KV, by placing the powder on a copper grid to observe the morphology, crystal structure

\*Corresponding author:  
Tel : +82-53-810-2334  
Fax: +82-53-810-4616  
E-mail: keel@ynu.ac.kr

and size of the powders. Fourier transform infrared spectra (FTIR) were measured on a Nicolet Impact 410 DSP spectrophotometer using the KBr pellet method.

## Results and Discussion

The thermal behavior of the precursor at  $R=4$  determined by TG-DTA in an oxygen atmosphere up to  $1000\text{ }^\circ\text{C}$  at a heating rate of  $10\text{ }^\circ\text{C min}^{-1}$  is shown in Figs.1 and 2. Decomposition started below  $200\text{ }^\circ\text{C}$  with a weight loss (15.7%) corresponding to the adsorbed water. In the temperature region between  $200\text{--}400\text{ }^\circ\text{C}$ , the main decomposition occurs with a weight loss in the range 24.2%. The thermal decomposition behavior is associated with exothermic effects in the DTA curve. The exothermic peak in the temperature range  $200\text{--}400\text{ }^\circ\text{C}$  in the DTA curve is due to the burning off of the residual surfactant. A final weight loss of (2.1%) on the TG curve was observed in the temperature range of  $500\text{--}1000\text{ }^\circ\text{C}$ . No clear exothermic peak indicating a transformation temperature to  $\text{CuAl}_2\text{O}_4$  was observed.

The XRD patterns of the precursor powders calcined in air at  $800\text{ }^\circ\text{C}$  for 2 h are shown in Fig. 3. According to

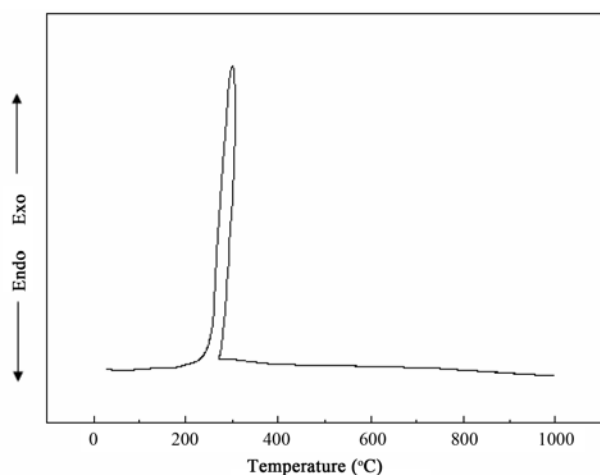


Fig. 1. DTA curve of  $\text{CuAl}_2\text{O}_4$  precursor powders at  $R=4$ .

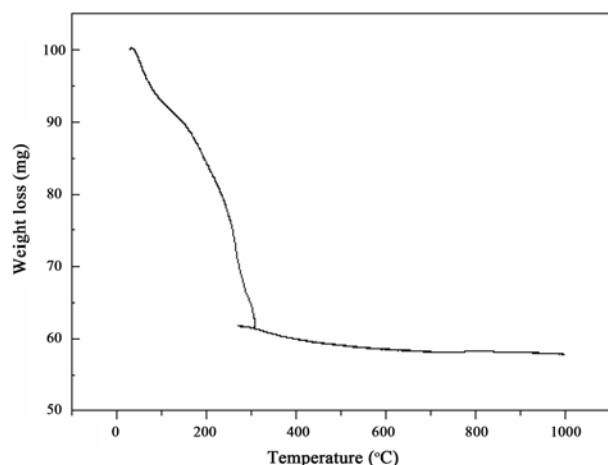


Fig. 2. TGA curve of  $\text{CuAl}_2\text{O}_4$  precursor powders at  $R=4$ .

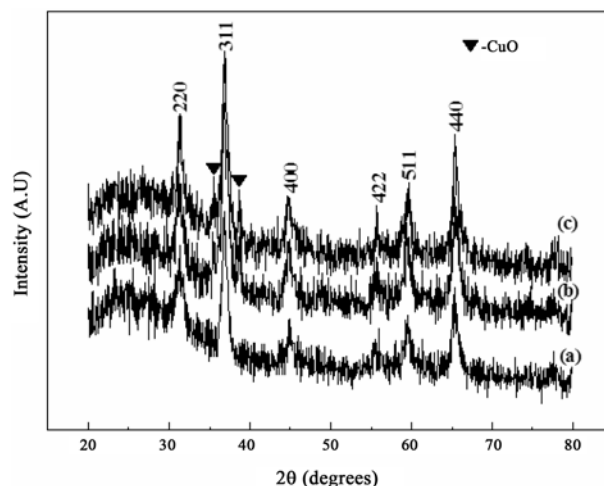


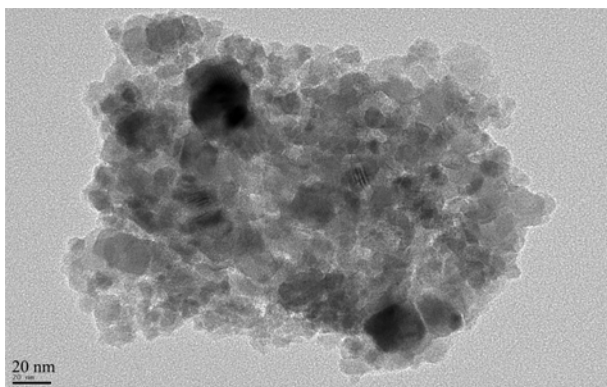
Fig. 3. XRD patterns of  $\text{CuAl}_2\text{O}_4$  precursor powders calcined at  $800\text{ }^\circ\text{C}$  (a)  $R=4$ ; (b)  $R=6$ ; (c)  $R=8$ .

Table 1. The crystallite size of  $\text{CuAl}_2\text{O}_4$  at  $1000\text{ }^\circ\text{C}$

$R = [\text{water}]/[\text{surfactant}]$	Crystallite size (nm)
4	25
6	30
8	33.8

the XRD analysis, the diffraction pattern at  $R=4$  shows the formation of the fully-crystalline, single phase  $\text{CuAl}_2\text{O}_4$ . All the diffraction lines in these XRD spectra could be attributed to the  $\text{CuAl}_2\text{O}_4$  phase having the perovskite crystal structure (PDF [78-1605]). With a further increase in the water-to-surfactant ratio ( $R$ ), a trace amount of  $\text{CuO}$  is found along with the  $\text{CuAl}_2\text{O}_4$  phase. The crystallite size of the synthesized powder calcined at  $800\text{ }^\circ\text{C}$  for different values of  $R$  was estimated from the X-ray line broadening of the (311) diffraction peak using the Scherrer formula [13]. Table 1 shows that the water/surfactant molar ratio ( $R$ ) influenced the crystallite size. It was reported that the size of the particles formed in reverse micelles is larger than the hydrodynamic size of the reverse micellar droplets, which is affected by the temperature and micellar size [14]. Moreover by increasing the water-to-surfactant ratio, one would expect that the nanoparticles would become bigger [14]. Many studies of nanoparticle formation in the reverse micelle process have been based on a two-step model [15-17]. The first step is nucleation. The second step is growth via reagent exchange between the micelles. The nucleation and growth are controlled by interaction between the micelles, and they can also be affected by the phase behavior and solubility, average occupancy of reacting species in the aqueous medium, dynamic behavior of the reverse micellar solution etc.

Figs. 4 and 5 show a TEM micrograph and a selected area diffraction pattern of powder synthesized at  $800\text{ }^\circ\text{C}$  for 2 h. The TEM micrograph shows that the crystallite size of the calcined powder is in the range  $10\text{--}20\text{ nm}$ . The selected area electron diffraction pattern (SAED), shown in Fig. 5, exhibits five broad rings which could be attributed to (220),



**Fig. 4.** TEM micrograph of  $\text{CuAl}_2\text{O}_4$  powders synthesized at  $800^\circ\text{C}$  with  $R = 4$ .

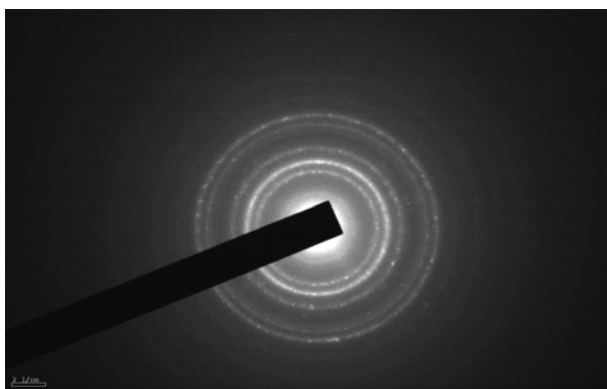


**Fig. 5.** Selected area diffraction (SAD) pattern of  $\text{CuAl}_2\text{O}_4$  powders synthesized at  $800^\circ\text{C}$  with  $R = 4$ .

(311), (400), (422) and (511) reflections of the copper aluminate spinel structure. The broadening of the diffraction rings suggests that the particles are small and/or are of low crystallinity. The HRTEM micrograph of Fig. 6 shows more clearly the rows of diffraction points, which are characteristics of the crystalline lattice. A comparison of the interplanar distances measured between the rows of diffraction points with those of the JCPDS cards indicates the presence of  $\text{CuAl}_2\text{O}_4$  with a spinel structure (PDF [78-1605]). The interplanar distance between rows of diffraction point is 0.283 nm which corresponds to the (220) plane.

To monitor the elimination of residual oil and surfactant phases from the micro emulsion-derived precursor and calcined powder at  $R = 4$ , spectroscopic analysis using FTIR was conducted on the as-dried powders and those calcined at  $800^\circ\text{C}$  for 2 h (Fig. 7). The broad vibrational band centered around  $3436\text{ cm}^{-1}$  and absorption band in the region  $2384\text{ cm}^{-1}$  indicates the presence of molecular water and  $\text{CO}_2$  absorption. The band intensities related to the hydroxyl group and  $\text{CO}_2$  band is still visible in the calcined sample. This may be due to moisture absorption during testing. The absorption band at  $2964\text{ cm}^{-1}$  is related to stretching C-H vibration from the organic compounds used in the synthesis. The infrared spectrum of a carboxyl group,  $\text{COO}^-$  shows the characteristic doublet absorption due to the asymmetric  $[\nu_{\text{as}}(\text{COO}^-)]$  and



**Fig. 6.** TEM micrograph of  $\text{CuAl}_2\text{O}_4$  powder synthesized at  $800^\circ\text{C}$  with  $R = 4$ .

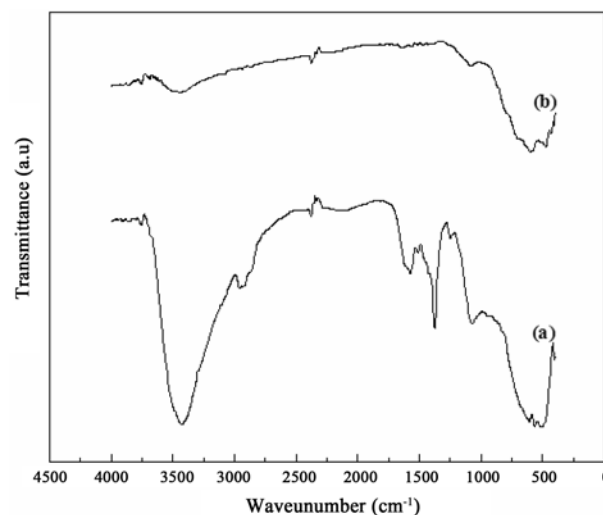


**Fig. 7.** FTIR analysis of  $\text{CuAl}_2\text{O}_4$  powders synthesized at  $R = 4$  (a) dried; (b) calcined at  $800^\circ\text{C}$ .

symmetric  $[\nu_{\text{s}}(\text{COO}^-)]$  stretching vibration at  $1577$  and  $1387\text{ cm}^{-1}$ , respectively. The absorption bands at  $1249\text{ cm}^{-1}$  and  $1061\text{ cm}^{-1}$  are probably due to CH-OH stretching vibrations. In the  $1000\text{-}400\text{ cm}^{-1}$  region of the IR spectra the observed specific peaks may be attributed to the characteristic Al-O-Al vibrations in  $\text{CuAl}_2\text{O}_4$  [12]. However, the calcined sample does not suggest the total elimination of water and organics. The presence of organics in the calcined sample provides a unique and desirable situation in limiting the growth of the crystallite sizes from unnecessary enlargement.

## Conclusion

The preparation and characterization of  $\text{CuAl}_2\text{O}_4$  nanoparticles in a water/Igepal CO 520/cyclohexane reverse micelle solution have been studied. The formation of the  $\text{CuAl}_2\text{O}_4$  phase was related to the water: surfactant ratio ( $R$ ). Phase pure  $\text{CuAl}_2\text{O}_4$  was synthesized at  $800^\circ\text{C}$  for 2 h at  $R = 4$ . The average particle size as determined from TEM varies from 10-20 nm.

### Acknowledgement

This research was supported by the Yeungnam University research grants.

### References

1. H.J. Woelk, B. Hoffmann, G. Mestl and R. Schloegl, *J. Am. Ceram. Soc.* 85 (2002) 1876-1878.
2. Alejandre, F. Medina, X. Rodriguez, P. Salagre and J.E. Sueiras, *J. Catal.* 188 (1999) 311.
3. T.W. Kim, M. Kang, H.L. Koh and K.L. Kim, *J. Chem. Eng. Jpn.* 34 (2001) 221-226.
4. K. Shimizu, H. Maeshima, H. Yoshida, A. Satsuma and T. Hattori, *Phys. Chem. Chem. Phys.* 2 (2000) 2435-2439.
5. M.C. Marion, E. Garbowski and H. Primet, *J. Chem. Soc., Faraday Trans.* 86 (1990) 3027-3032.
6. F. Mayer, R. Hempelmann, S. Mathur and M. Veith, *J. Mater. Chem.* 9 (1999) 1755-1763.
7. T. Sugimoto, K. Kimijima and J. Phys. Chem. B. 107 (2003) 10753-10759.
8. M.C. McLeod, R.S. McHenry, E.J. Beckman and C.B. Roberts, *J. Phys. Chem. B.* 107 (2003) 2693-2700.
9. W. Sun, L. Xu, Y. Chu and W. Shi, *J. Colloid Interface Sci.* 266 (2003) 99-106.
10. M. Boutonnet, J. Kizling, P. Stenius and G. Maire, *Colloids Surf.* 5 (1982) 209-225.
11. T. James, M. Padmanabhan, K.G.K. Warriar and S. Sugunan, *Mater. Chem. Phys.* 103 (2007) 248-254.
12. J. Yanyan, L. Jinggang, S. Xiaotao, N. Guiling, W. Chengyu and G. Xiumei, *J. Sol-Gel Sci. Technol.* 42 (2007) 41-45.
13. M.P. Klug and L.E. Alexander, *X-ray Diffraction procedure for polycrystalline and amorphous materials*, Wiley: New York, 1974.
14. N. Munshi, T.K. De and A.N. Maitra, *J. Colloid Interf. Sci.* 190 (1997) 387-391.
15. T.F. Towey, A. Khan-Lidhi and B.H. Robinson, *J. Chem. Soc. Faraday Trans.* 86 (1990) 3757-3762.
16. R. Bandyopadhyaya, R. Kumar, K.S. Gandhi and D. Ramkrishna, *Langmuir* 13 (1997) 3610-3620.
17. M.A. Lopez-Quintela, J. Rivas, *J. Colloid Interf. Sci.* 158 (1993) 446-451.